



## Numerical Modeling of Rock Slopes with a Potential of Block-Flexural Toppling Failure

H. Sarfaraz\* and M. Amini

*School of Mining Engineering, College of Engineering, University of Tehran, thehram, Iran*

Received 5 September 2019; received in revised form 7 November 2019; accepted 14 November 2019

### Keywords

*Rock Slopes*

*Block-Flexural Toppling*

*Numerical Modeling*

*Distinct Element Method*

### Abstract

One of the most important instabilities of rock slopes is toppling failure. Among the types of toppling failure, block-flexural failures are a more common instability, which occurs in nature. In this failure, some rock blocks break due to tensile stresses, and some overturn under their weights, and next to all of them topple together. In 2015, the physical and theoretical modeling of this failure has been studied by Amini *et al.* Due to the complexity of this failure mechanism, no appropriate numerical model has been proposed so far. In this research work, first, a literature review of the toppling failure is summarized. Then using the UDEC software, as a distinct element method (DEM), the experimental models are analyzed numerically, and the Voronoi joint model is applied to simulate the failure. The results of the numerical simulations are compared with the outcomes of the physical models and analytical solutions. This comparison illustrates that the numerical modeling has a good agreement with the corresponding experimental tests and theoretical approaches. Also the results obtained show that although the mechanism of block-flexural toppling failure is complicated, the numerical code is well-capable of analyzing this failure.

### 1. Introduction

Toppling failure is a frequent instability in natural and human-made rock slopes. From a mechanical viewpoint, the primary toppling failure is categorized as flexural, blocky, and block-flexural [1]. If a rock mass is made up of a series of parallel discontinuities, dipping steeply against the facing slope, it will act like some rock columns that are placed on top of each other. In this case, rock columns are under tensile and compressive bending stresses due to their own weights. If the maximum tensile stress in every rock column surpasses its tensile strength, it fails and topples. Such an instability is classified as the flexural toppling failure (Figure 1-A). If one cross-joint series is added to the rock mass (Figure 1-B), the system

cannot withstand the tensile bending stress, and consequently, the columns may overturn due to their weights. This type of failure is regarded as a typical blocky toppling failure. In real case histories, the above-mentioned perfect cases are rarely encountered, and toppling failure is mostly of block-flexural (Figure 1-C). This instability is a combination of the blocky and flexural toppling failure modes. Many research articles are available on the flexural and blocky toppling failures [2].

In this work, first, the theoretical method and physical modeling of Amini *et al* [4] are reviewed. Then the experimental tests are examined through a numerical simulation using the UDEC software, and the results obtained are discussed.

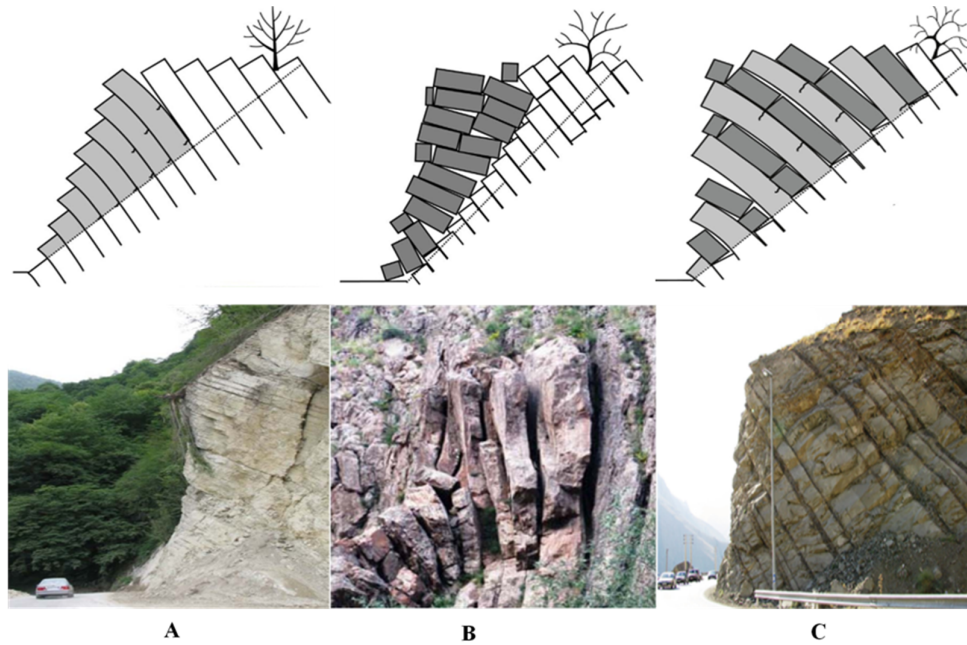


Figure 1. Schematic diagrams and real case studies of primary toppling failure: A) flexural, B) Blocky, C) Block-Flexural [3, 5].

## 2. Literature Review

Müller [6] was the first who mentioned the overturning of rock blocks in 1968. He suggested that block toppling or rotation may have an effective factor in the failure of the north face of the Vaiont slide. In 1971, Ashby [7] analyzed the rotation of rock columns and presented some criteria based on the theoretical and experimental tests. Also Ashby recommended the appointment of “toppling” for such failures. In 1970, Erguvanli and Goodman [8] introduced a physical model to study the toppling failure through a base friction table apparatus. Goodman and Bray classified the toppling failure into the primary (flexural, blocky, and block-flexural) and secondary types [1]. For the primary type of toppling failures, the weight of the rock mass is the governing factor of the instability. Secondary toppling failure is stimulated by some external factors, and is entirely various. Some studies have been carried out for these types of failures [3, 5, 9-15]. In 2019, Sarfaraz et al. [16] numerically modeled the slide-head-toppling failure using the finite element method, and illustrated acceptable agreements with the pre-existing physical modeling and analytical approach results.

From 1976 till now, many physical tests, numerical modelings, analytical methods, design charts, and case studies of toppling failure have been published based on the Goodman and Bray classification [17-22]. Aydan and Kawamoto [23,24] modeled the

toppling failure of the rock slopes, employing a friction table apparatus during 1987 and 1992. In 1993, Shimizu *et al.* [25] modeled some examples of the flexural toppling failure with finite element and discrete element methods. Adhikary *et al.* [26] modeled the flexural toppling failure using a geotechnical centrifuge apparatus in 1997. In 2007, Adhikary and Dyskin [27] conducted a new series of centrifugal model tests, where glass and concrete samples with the potential of flexural toppling were used as the materials. For the study of the kinetic conditions in toppling failure, Yeung and Wong [28] conducted a physical modeling and a 3D discontinuous deformation analysis. Based on the governing compatibility principles of cantilever beams, Amini *et al.* presented a straightforward solution for the stability analysis of flexural toppling failure [29, 30]. Also in 2012, Amini *et al.* [2] combined the method of Goodman and Bray with the method of Aydan and Kawamoto for the analysis of block-flexural toppling failure. In 2018, Zheng *et al.* [30] suggested a theoretical solution for rock slopes against sliding or flexural-toppling failure based on the limit equilibrium theory and two experimental model tests. Furthermore, they investigated the mechanisms of flexural toppling failure using the limit equilibrium theory and numerical modeling [32]. In 2019, Liu *et al.* [33] employed a 3D-DDA analysis method to analyze the toppling failure.

### 3. A review of theoretical method for block-flexural toppling failure

Amini *et al.* [4] proposed an analytical approach to analyze and calculate the value of the safety factor of block-flexural toppling failure on the basis of the equilibrium and compatibility laws; this method is identified as the equivalent length ( $\psi$ ) approach. The parameter  $\psi$  can be computed as follows [4]:

$$\psi = \frac{-B \pm (B^2 - 4AC)^{0.5}}{2A}$$

$$A = \frac{\tan(\delta - \varphi \pm \beta) \cos^2 \varphi}{\tan(\delta - \varphi \pm \beta) + \tan(\theta - \delta + \varphi)}$$

$$B = \frac{2 \cos(\theta - \delta + \varphi) \cos \varphi}{\sin \theta} H$$

$$C = \left[ \frac{\cos(\theta - \delta + \varphi)}{\sin \theta} H \right]^2 \quad (1)$$

where,

- $\psi$  : Equivalent length of rock slope (meter);
- $\delta$  : Angle of rock mass stratification with respect to the horizontal (degree);
- $\varphi$  : Angle between overall failure plane and the line of normal discontinuities (degree);
- $\beta$  : Angle of upper surfaces of rock slopes with respect to the horizontal (degree);
- $\theta$  : Angle of face slope with respect to the horizontal (degree);
- $H$  : Slope height (meter).

These parameters are shown in Figure 2. The value of the safety factor for the flexural toppling failure can be obtained as follows [4]:

$$F_s = \frac{t\sigma_t}{3\psi^2 \gamma \cos \delta} \quad (2)$$

Also the safety factor of the block with the equivalent length  $\psi$  for block toppling failure can be calculated as follows [4]:

$$F_s = \frac{t}{\psi \tan \delta} \quad (3)$$

In block-flexural toppling failures, the blocks with the potential of toppling failure exert part of their weight force on the cantilever rock column. Accordingly, it is recommended that a combination of the above relationships is used to analyze the rock slopes against block-flexural toppling failure [4]:

$$F_s = k \frac{t}{\psi \tan \delta} + (1-k) \frac{t\sigma_t}{3\psi^2 \gamma \cos \delta} \quad (4)$$

in which the parameter  $k$  is a dimensionless correction factor that differs between 0 and 1; this factor indicates the percentage of blocks with a pure blocky potential compared to all blocks in the rock slopes. If all of the blocks are cantilevers under flexure, the slope will be capable of a pure flexural toppling failure, so this coefficient is equal to 0; else, it will be less than 1. Furthermore, if all the blocks have the potential of blocky toppling, this coefficient will be equal to 1 [4].

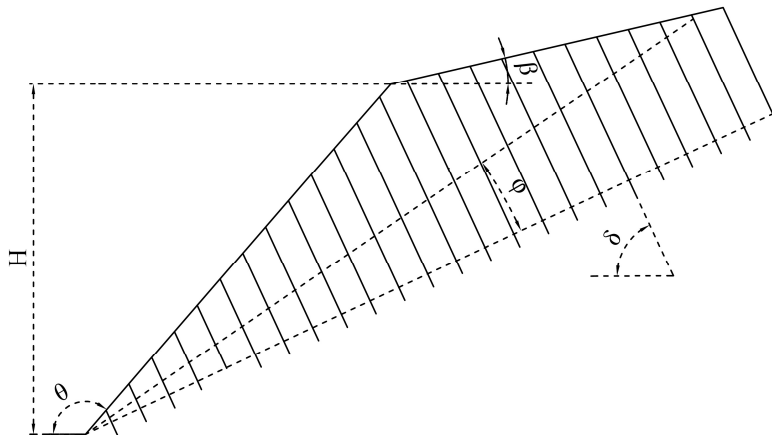


Figure 2. A schematic figure of rock slope with a prone of toppling failure.

### 4. Modeling of block-flexural toppling failure

#### 4.1. A review of physical modeling

Base friction, tilting table, and centrifuge apparatus are conventional geotechnical methods used to study the behavior of soil and rock structures.

Amini *et al.* [4] conducted physical models using a tilting table device (Figure3) that had a box placed over a pneumatic jack to set up the models. The columns used for the physical models of a single

column and layered rock slopes were created through the consolidation of a special mixture consisting of BaSO<sub>4</sub>, ZnO, and Vaseline oil under a chosen pressure. The jack gradually increases the table angle, and the dip of the blocks and the slope angle vary proportionately. The other components in the tilting table include the air compressor, air-

transfer hoses, compressed air fitting and fasteners, table's angular velocity control equipment, and devices to read the table slope. After adjusting the model, the table is tilted until a failure happens. Hence, the angle at which the model initiates to fail or slide can be considered as the angle of instability [4].

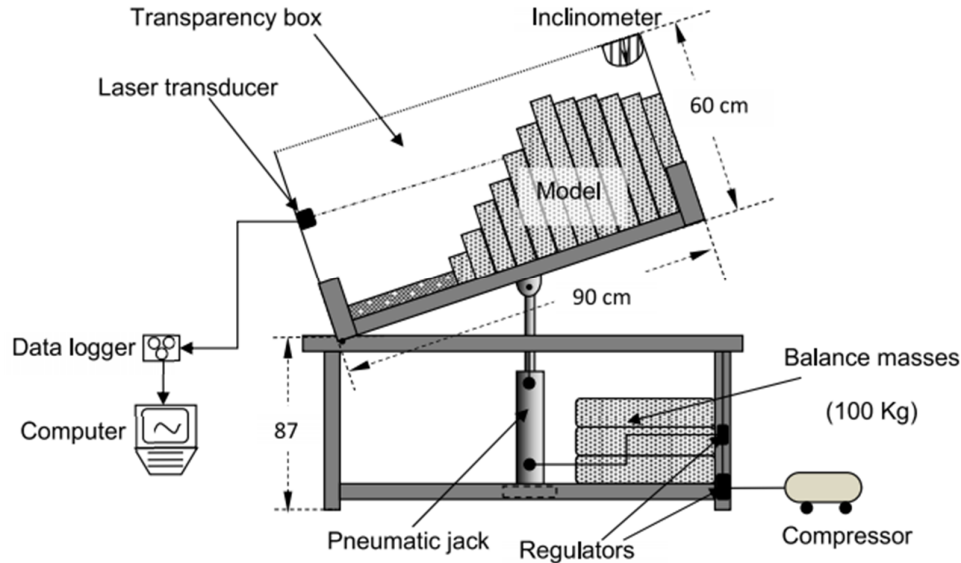


Figure 3. A schematic representation of the tilting table machine used for physical modeling [4].

#### 4.2. Numerical modeling

Numerical methods are commonly used as the tools for solving many problems of rock mechanics. The results of the physical models are simulated using the numerical software UDEC. This software is a 2D numerical program based on the distinct element method for discontinued media, for instance, rock slopes, toppling failure, and crack propagation. This software is based on the Lagrangian computational technique, which is suitable for simulating the movements and distortion of a block scheme. The discontinuities are treated as boundary conditions between blocks,

and they are allowed large displacement alongside discontinuities and rotations of blocks [34]. For numerical modeling, the physical and mechanical properties of the materials should be available. The block properties are presented in Table 1. Also the properties of the joints between blocks are listed in this Table. The Mohr-Coulomb criterion was used in the numerical modeling. The Voronoi model (internal flaws) was applied to simulate the failure in which the parameters of this model were similar to the geo-mechanical parameters of the blocks.

Table 1. Parameters of numerical model [4].

Model parameters	Blocks	Internal flaws	Joint element
Unit weight (kN/m <sup>3</sup> )	23.4	-	-
Modulus of elasticity (MPa)	7	-	-
Poison ratio	0.25	-	-
Tensile strength (kPa)	31	31	0
Cohesion (kPa)	15	15	0
Friction angle (degree)	35	35	30
Normal stiffness (MPa/m)	-	50	20
Shear stiffness (MPa/m)	-	5	2

Amini *et al.* [4] modeled the block-flexural toppling in two sections. In the first step, ideally, it

was supposed that the geometries of the slope block were divided into two portions as blocky and

flexural so that each other block was possibly blocky or flexural. However, these models are actually different from real rock slopes since slope blocks are frequently arranged randomly in nature. Thus in the second section, the random patterns are modeled to be more similar to the real layered rock slopes. In both sections, after the models were built, the table slowly tilted to cause failure to happen. Parameters such as the table angle and angle of overall plane failure were measured [4]. In the numerical modeling, the models were prepared at the angle at which the physical models initiated to fail or slide that could be considered as the instability angle. Next, the models were analyzed by the shear strength reduction method. In the following section, these two series of modeling are explained separately. Pictures of all the physical and numerical models (tests 1 to 8) are shown in

the appendix at the moment of the failure. The tests 1 and 2 are for an ideal block-flexural toppling failure. Also the tests 3 to 8 are for a non-ideal block-flexural toppling failure.

**4.2.1. Modeling ideal block-flexural toppling failure**

In Figure 4, an example of these physical models is shown before testing and during failure. In these models, in fact, two consecutive blocks are similar to the two-block models; one block is fixed at its pivot, and is capable of carrying tensile stresses but the next block is free at its end and imposes its weight, after the table tilts, on the fixed block. Due to some constraints on the construction and movement of the blocks, two physical models were performed [4]. The modeling results are displayed in Table 2.

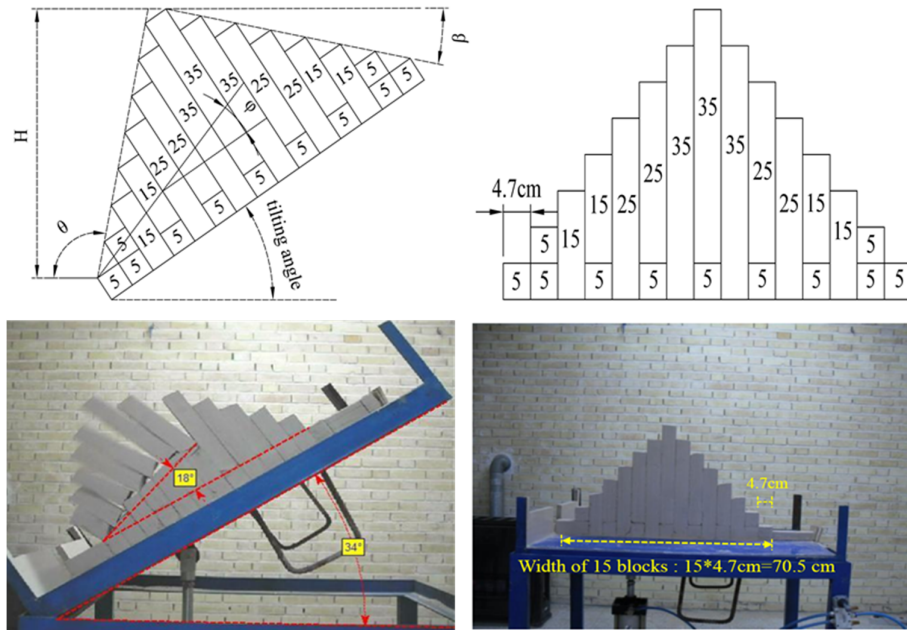


Figure 4. Physical modeling of ideal block-flexural toppling failure (Test 1) [4].

Table 2. Geometrical parameters of ideal block-flexural toppling failure with physical modeling [4].

Test No.	$\beta$ (°)	$\varphi$ (°)	$\delta$ (°)	$\theta$ (°)	H (cm)
1	-13	18	56	99	47.44
2	-5	26	48	91	37.45

Figure 5 shows the numerical analysis results corresponding to the physical model of Test 1. The stress reduction factor of this model is equal to 0.975. In Figure 5, the symbols (°) and (\*) illustrate the tensile and yield points, respectively. As it can be seen in this figure, the rock blocks have failed under the tensile stresses. Furthermore, distribution of the displacement vector is presented in this figure. According to this figure, the angle between

the normal to discontinuities and overall toppling failure plane is 20° in the numerical modeling, which has an acceptable agreement with the corresponding physical model. Also the results of numerical models presented in Table3 at the angle that the SRF value is equal to one. It is believed that in numerical methods, this value of critical stress reduction factor can be assumed to be equivalent to a safety factor [5].

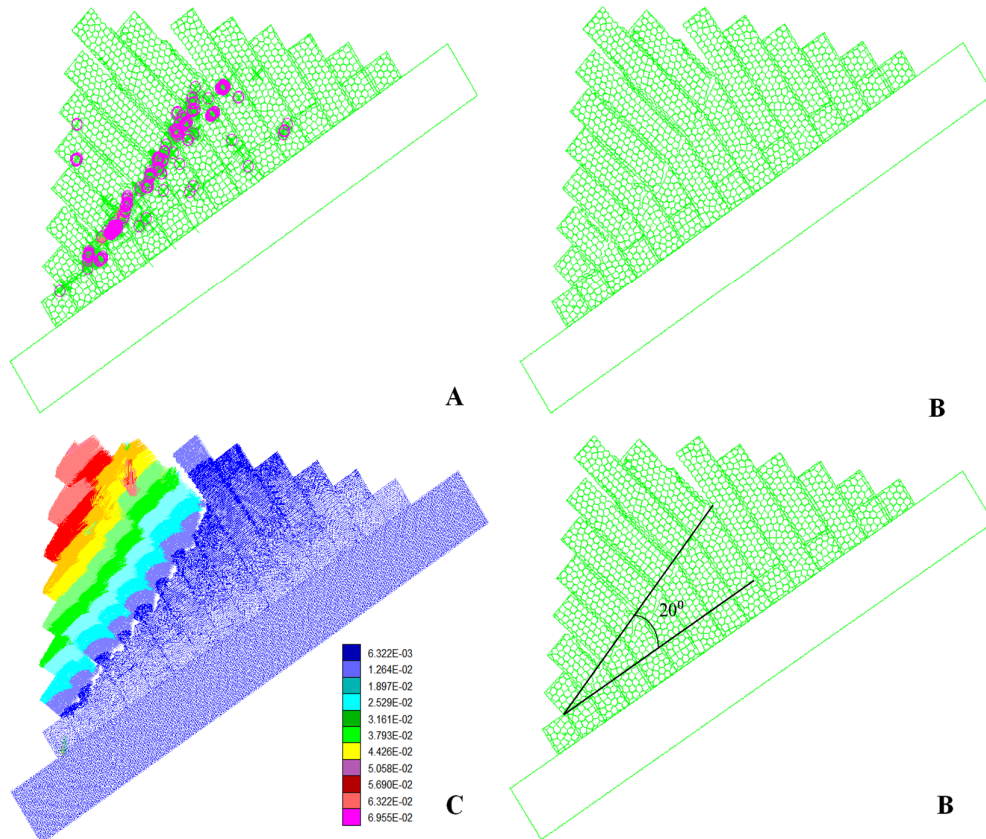


Figure 5. Numerical modeling of ideal block-flexural toppling failure (Test 1): A) Plot of Plastic, B) Plot of Block, C) Plot of the displacement vector (the unit of the displacement vector is m/s)

Table 3. Geometrical parameters of ideal block-flexural toppling failure with physical modeling.

Test No.	$\beta$ (°)	$\varphi$ (°)	$\delta$ (°)	$\theta$ (°)	H (cm)
1	-14	20	57	100	47.27
2	-7	22	50	93	37.28

#### 4.2.2. Modeling of random set up of block-flexural toppling failure

In the second section, the blocks were placed entirely randomly in the model so that some of them were broken and the others were overturned freely. By choosing a random set of length blocks, the models fail against the block-flexural toppling

failure. This behavior is almost similar to the actual rock slopes in which the rock columns are randomly bent or overturned [4]. The schematic view and photograph of the model from these experiments are shown in. Figure 6. The results of the modeling can be seen in Table 4.

Table 4. Geometrical parameters of block-flexural toppling failure with random set-up by physical modeling [4].

Test No.	$\beta$ (°)	$\varphi$ (°)	$\delta$ (°)	$\theta$ (°)	H (cm)
3	-26	15	69	112	44.46
4	-18	27	61	104	46.56
5	-21	30	64	107	45.88
6	-12	29	55	98	47.54
7	-26	34	69	112	44.46
8	-22	22	65	108	45.62

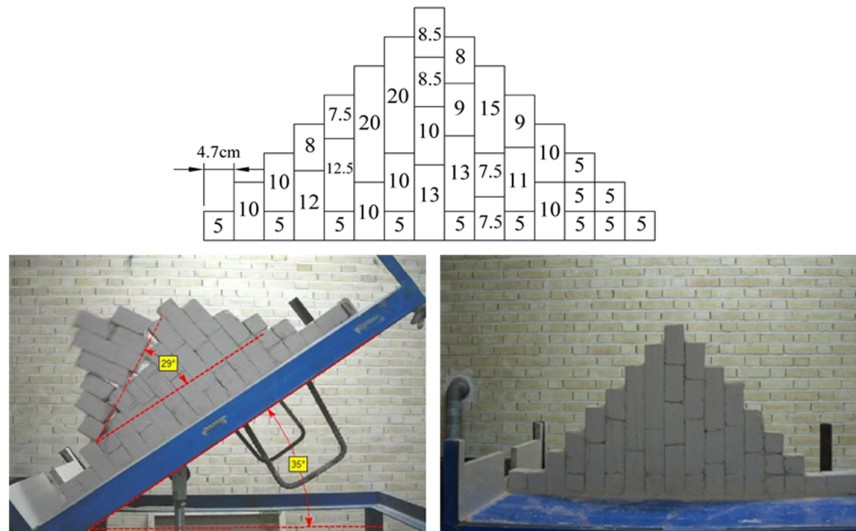


Figure 6. Physical modeling of block-flexural toppling failure (Test 6) [4].

The results of numerical modeling such as plastic points and distribution of displacement vector of Test 6 (Figure 6) are shown in Figure 7. According to this figure, some blocks were broken under the tensile stress (flexural portion), and the others were separated along the secondary joint (blocky

portion), causing a general toppling failure. The failure pattern of the numerical model is in a reasonable agreement with the corresponding physical model. Furthermore, the results of the tests 3 to 8 at the moment of failure are presented in Table 5.

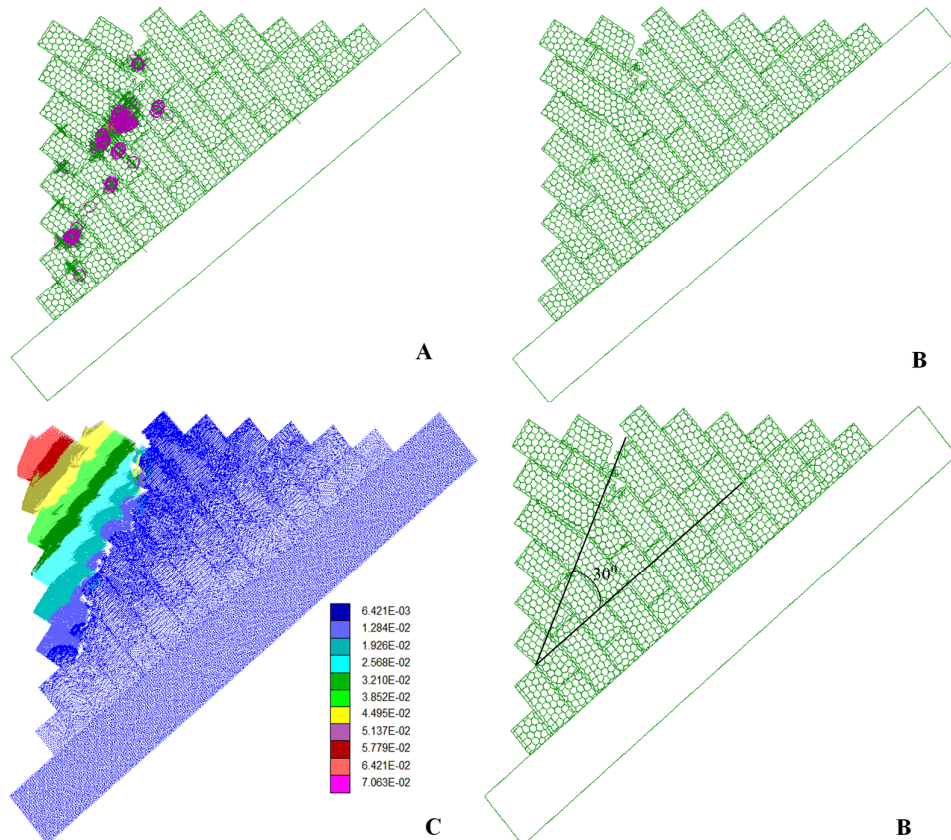


Figure 7. Numerical modeling of block-flexural toppling failure (Test 6) (unit of the displacement vector is m/s).

**Table 5. Geometrical parameters of block-flexural toppling failure with random set-up by numerical modeling.**

Test No.	$\beta$ (°)	$\varphi$ (°)	$\delta$ (°)	$\theta$ (°)	H (cm)
3	-29	23	72	115	43.46
4	-22	19	65	108	45.62
5	-22	24	65	108	45.62
6	-10	30	53	96	47.75
7	-24	24	67	110	45.07
8	-24	25	67	110	45.07

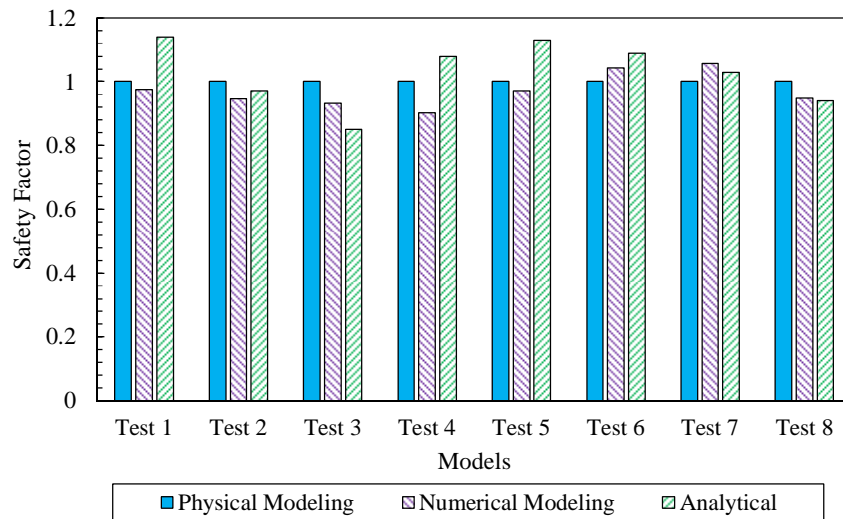
### 4.3. Results and discussion

In this section, the results of the numerical modeling were compared with the corresponding physical models and analytical method. As it can be seen in Figures 4 to 7 and also Table 2 to 5, by comparing the geometrical parameters and how the blocks are toppling, the numerical modeling has a good agreement with the physical modeling. Additionally, the most appropriate quantity for comparison between these models is the value of the critical stress reduction factor. Since the value of the safety factor of the physical model is equal to 1 at the moment of failure, the critical stress reduction factor of the numerical model must also

be equal to 1. In Table 6, the stress reduction factor of the numerical models is compared with the safety factor of the physical models. The differences between the numerical and physical results are less than 10%, which appear to be reasonable due to the complexity of the failure mechanism. It is also possible to compare the values for the safety factor obtained from the numerical and physical models with the values for the safety factor obtained from the theoretical solution proposed by Amini *et al.* (relationships 1 to 4). The results of this comparison are presented in Figure 8.

**Table 6. Comparison of the numerical modeling results with the corresponding physical models.**

Models	Test 1	Test 2	Test 3	Test 4	Test 5	Test 6	Test 7	Test 8
$F_s$ in physical modeling	1	1	1	1	1	1	1	1
SRF in numerical modeling	0.974	0.946	0.932	0.903	0.971	1.042	1.057	0.948
Difference (%)	2.6	5.4	6.8	9.7	2.9	4.2	5.7	5.2

**Figure 8. Comparison of the safety factor in numerical modeling and analytical methods with the corresponding physical model.**

### 5. Conclusions

In this work, the mechanism of the block-flexural toppling failure was examined through a series of numerical models, analyzed using the UDEC software as a distinct element code. The physical

and theoretical modeling of this failure was investigated by Amini *et al.* in 2015. In this numerical modeling, for simulating a failure, the Voronoi joint model was applied. In the ideal

models, the number of blocks having a potential of block toppling failure is equal to the number of blocks having a potential of flexural toppling failure, and the failure plane is such that half the blocks are broken under tensile stresses. However, in non-ideal models, the number of blocks with the potential of blocky and flexural toppling failure is not necessarily the same, and the failure plane is formed so that fewer blocks are broken under tensile stresses due to blocks placed randomly. The results of numerical models were compared with the outcomes of the experimental tests and theoretical method. This comparison demonstrates that numerical modeling has a good agreement with the corresponding physical models, where the differences between the numerical and experimental results are less than 10%. Correspondingly, the results show that although the mechanism of block-flexural toppling failure is complex, the distinct element method is well-capable of analyzing the block-flexural toppling failure, and the UDEC software is an efficient tool for evaluating the stability analysis of this failure.

#### Conflicts of interest

The authors wish to confirm that there are no known conflicts of interest associated with this publication, and there has been no considerable financial support for this study that could have influenced its outcome.

#### Acknowledgement

The authors express their science thanks to Professor Ömer Aydan from Ryukyu University, Ryukyu, Japan, for his invaluable help and guidance throughout this research work.

#### References

[1]. Wyllie, D.C., Mah, C.W. and Hoek, E. (2004). *Rock slope engineering : civil and mining*. Spon Press.

[2]. Amini, M., Majdi, A. and Veshadi, M.A. (2012). Stability analysis of rock slopes against block-flexure toppling failure, *Rock Mech. Rock Eng.* 45 (4): 519-532.

[3]. Amini, M., Ardestani, A. and Khosravi, M.H. (2017). Stability analysis of slide-toe-toppling failure, *Eng. Geol.* 228: 82-96.

[4]. Amini, M., Golamzadeh, M. and Khosravi, M. (2015). Physical and theoretical modeling of rock slopes against block-flexure toppling failure. *Int. J. Min. Geo-Engineering*, 49 (2): 155–171.

[5]. Amini, M. and Ardestani, A. (2019) Stability analysis of the north-eastern slope of Daralou copper open pit mine against a secondary toppling failure, *Eng. Geol.* 249: 89-101.

[6]. Müller, L. (1968). New considerations on the Vaiont slide, *Rock Mech Eng Geol.* 6: 1-91.

[7]. Ashby, J. (1971). *Sliding and toppling modes of failure in models and jointed rock slopes*, Imperial College, University of London.

[8]. Erguvanli, R., Goodman, K. (1970). Applications of models to engineering geology for rock excavations. *Assoc Eng Geol.* 9 P.

[9]. Mohtarami, E., Jafari, A. and Amini, M. (2014). Stability analysis of slopes against combined circular-toppling failure. *Int. J. Rock Mech. Min. Sci.* 67:43-56.

[10]. Tsesarsky, M. and Hatzor, Y.H. (2009). Kinematics of overhanging slopes in discontinuous rock. *J. Geotech. Geoenvironmental Eng.* 135 (8): 1122-1129.

[11]. Frayssines, M. and Hantz, D. (2009). Modeling and back-analyzing failures in steep limestone cliffs. *Int. J. Rock Mech. Min. Sci.* 46 (7): 1115-1123.

[12]. Evans, R.S. (1981). An analysis of secondary toppling rock failures the stress redistribution method. *Q. J. Eng. Geol. Hydrogeol.* 14 (2): 77-86.

[13]. Nichol, S.L., Hungr, O. and Evans, S.G. (2002). Large-scale brittle and ductile toppling of rock slopes, *Can. Geotech. J.* 39 (4):773-788.

[14]. Alejano, L.R., Gómez-Márquez, I. and Martínez-Alegría, R. (2010). Analysis of a complex toppling-circular slope failure. *Eng. Geol.* 114 (1): 93-104.

[15]. Amini, M., Sarfaraz, H. and Esmaeili, K. (2018). Stability analysis of slopes with a potential of slide-head-toppling failure. *Int. J. Rock Mech. Min. Sci.* 112: 108-121.

[16]. Sarfaraz, H., Khosravi, M.H. and Amini, M. (2019). Numerical Analysis of Slide-Head-Toppling Failure, *J. Min. Environment*. In press.

[17]. Savigny, M.A.P.K.W. (1990). Numerical modelling of toppling, *Can. Geotech. J.* 4: 823-834.

[18]. Bobet, A. (2002). Analytical solutions for toppling failure. *Int. J. Rock Mech. Min. Sci.* 36 (7): 971-980.

[19]. Sagaseta, C., Sánchez, J.M. and Cañizal, J. (2001). A general analytical solution for the required anchor force in rock slopes with toppling failure. *Int. J. Rock Mech. Min. Sci.* 38 (3): 421-435.

[20]. Brideau, M.A. and Stead, D. (2010). Controls on block toppling using a three-dimensional distinct element approach. *Rock Mech. Rock Eng.* 3 (3): 241-260.

[21]. Babiker, A.F.A., Smith, C.C., Gilbert, M. and Ashby, J.P. (2014). Non-associative limit analysis of the toppling-sliding failure of rock slopes. *Int. J. Rock Mech. Min. Sci.* 71: 1-11.

[22]. Alejano, L.R., Carranza-Torres, C., Giani, G.P. and Arzúa, J. (2015). Study of the stability against

toppling of rock blocks with rounded edges based on analytical and experimental approaches, *Eng. Geol.* 195: 172-184.

[23]. Aydan, Ö. and Kawamoto, T. (1992). The stability of slopes and underground openings against flexural toppling and their stabilisation. *Rock Mech. Rock Eng.* 3 (3): 143-165.

[24]. Aydan, Ö. and Kawamoto, T. (1987). Toppling failure of discontinuous rock slopes and their stabilization (in Japanese). *J. Japan Min. Soc.* 103: 673-770.

[25]. Shimizu, T., Aydan, Y. and Kawamoto, Ö. (1993). Several toppling failures in Japan and their back analysis, in *Assessment and Prevention of Failure Phenomena*. in *Rock Engineering Conference*. 879-885.

[26]. Adhikary, D.P., Dyskin, A.V., Jewell, R.J. and Stewart, D.P. (1997). A study of the mechanism of flexural toppling failure of rock slopes. *Rock Mech. Rock Eng.* 30 (2): 75-93.

[27]. Adhikary, D.P. and Dyskin, A.V. (2007). Modeling of progressive and instantaneous failures of foliated rock slopes. *Rock Mech. Rock Eng.* 40 (4): 349-362.

[28]. Yeung, M.R. and Wong, K.L. (2007). Three-dimensional kinematic conditions for toppling, *Proc. 1st*

*Canada-US Rock Mech. Symp. Rock Mech. Meet. Soc. Challenges Demands*. 1: 335-339.

[29]. Majdi, A. and Amini, M. (2011). Analysis of geo-structural defects in flexural toppling failure. *Int. J. Rock Mech. Min. Sci.* 45 (2): 175-186.

[30]. Amini, M., Majdi, A. and Aydan, Ö. (2009). Stability analysis and the stabilisation of flexural toppling failure. *Rock Mech. Rock Eng.* 42 (5): 751-782.

[31]. Zheng, Y., Chen, C., Liu, T., Xia, K. and Liu, X. (2018). Stability analysis of rock slopes against sliding or flexural-toppling failure, *Bull. Eng. Geol. Environ.* 77 (4): 1383-1403.

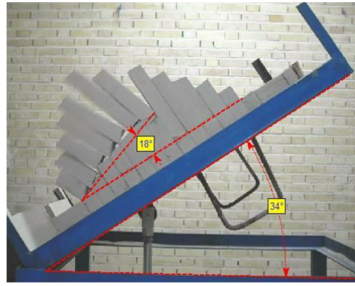
[32]. Zheng, Y., Chen, C., Liu, T., Zhang, H., Xia, K. and Liu, F. (2018). Study on the mechanisms of flexural toppling failure in anti-inclined rock slopes using numerical and limit equilibrium models. *Eng. Geol.* 237: 116-128.

[33]. Liu, G., Li, J. and Kang, F. (2019). Failure Mechanisms of Toppling Rock Slopes Using a Three-Dimensional Discontinuous Deformation Analysis Method. *Rock Mech. Rock Eng.* 1-24.

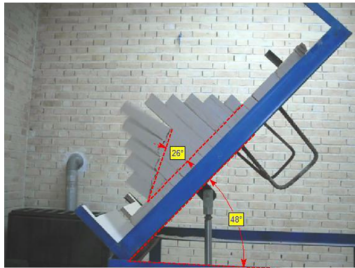
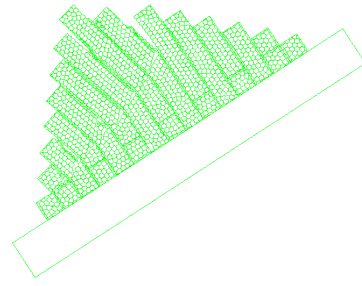
[34]. ITASCA Cons. (2014). ITASCA Cons. Group INC., UDEC code-vers. 6, Minneapolis-Minnesota.

**Appendix**

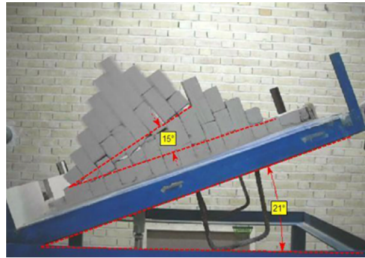
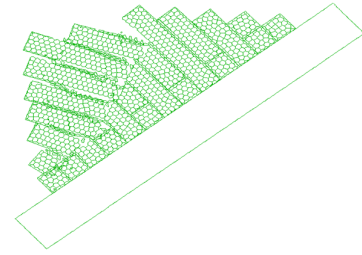
Pictures of all physical and numerical models at the moment of failure.



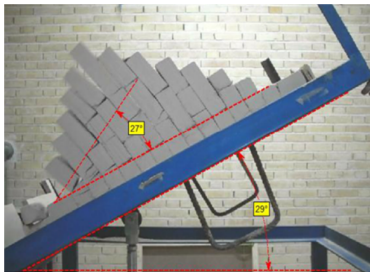
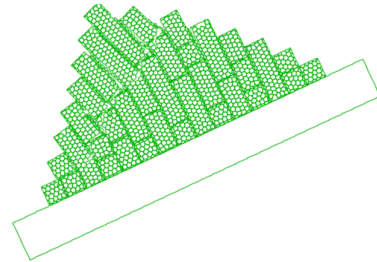
Test 1



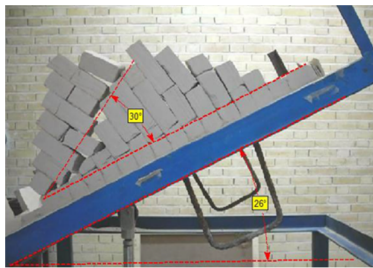
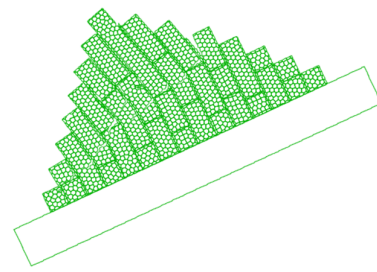
Test 2



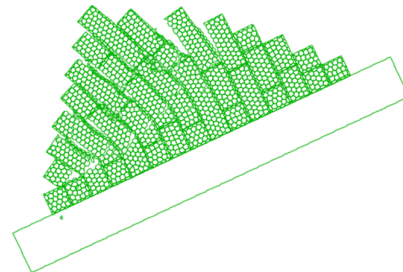
Test 3

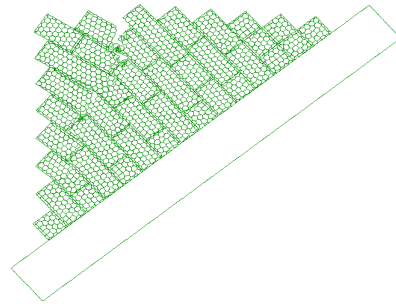
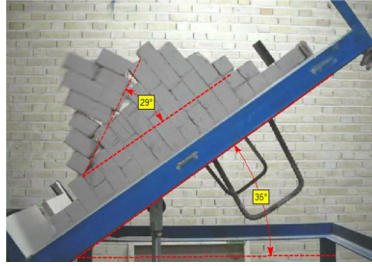


Test 4

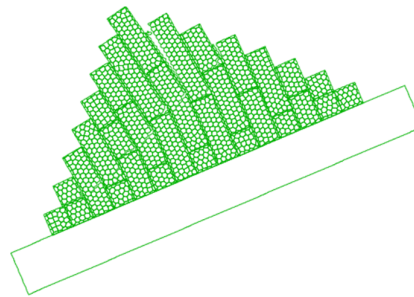
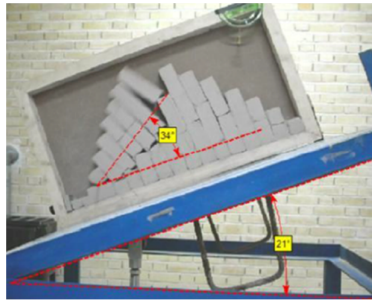


Test 5

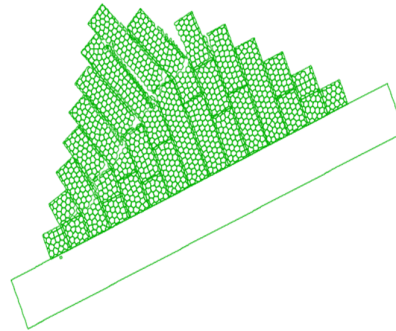
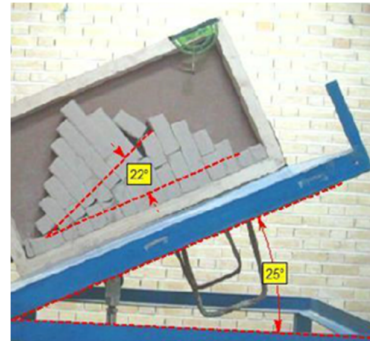




Test 6



Test 7



Test 8

## مدل سازی عددی شیروانی های سنگی با پتانسیل شکست واژگونی بلوکی - خمشی

حسن سرفراز<sup>1\*</sup>، مهدی امینی<sup>1</sup>

1- گروه مکانیک سنگ، دانشکده مهندسی معدن، دانشکده فنی دانشگاه تهران، تهران، ایران

ارسال 2019/9/05، پذیرش 2019/11/14

\* نویسنده مسئول مکاتبات: sarfaraz@ut.ac.ir

---

### چکیده:

یکی از مهم ترین ناپایداری ها در شیروانی های سنگی، شکست های واژگونی است. از میان انواع شکست های واژگونی، شکست واژگونی بلوکی - خمشی در طبیعت بیشتر مشاهده می شود. در این شکست، بعضی از بلوک ها در اثر خمش شکسته شده و برخی دیگر آزادانه حول پاشنه خود می چرخند و در نهایت همه آن ها با یکدیگر واژگون می شوند. در سال 2015، مدل سازی فیزیکی و تحلیلی این نوع شکست توسط امینی و همکاران مطالعه شد. به دلیل پیچیدگی مکانیسم این نوع شکست، تاکنون مدل عددی مناسبی پیشنهاد نشده است. در این تحقیق، ابتدا تاریخچه کوتاهی از شکست های واژگونی ارائه می شود. سپس با استفاده از نرم افزار المان مجزای UDEC، مدل های آزمایشگاهی مدل سازی عددی شدند و مدل موزاییکی (Voronoi) برای شبیه سازی شکست بکار گرفته شد. نتایج بدست آمده از مدل سازی عددی با نتایج مدل سازی فیزیکی و تحلیلی مقایسه شد. این مقایسه نشان می دهد که مدل های عددی تطابق قابل قبولی با مدل های آزمایشگاهی متناظر و روش تحلیلی دارد. همچنین نتایج بدست آمده نشان داد که اگرچه مکانیسم شکست واژگونی بلوکی - خمشی پیچیده است، مدل عددی پیشنهادی، ابزار مناسبی برای تحلیل و پیش بینی رفتار این نوع شکست است.

**کلمات کلیدی:** شیروانی سنگی، شکست واژگونی بلوکی - خمشی، مدل سازی عددی، روش المان مجزا.

---